

Article

Optimization of Controlled Low-Strength Material from Multi-Component Coal-Based Solid Waste

Tianxiang Chen, Ning Yuan *, Shanhu Wang, Xinling Zhang, Chaoyang Lin, Xinyue Wu, Qibao Wang and Dongmin Wang

School of Chemical and Environmental Engineering, China University of Mining and Technology, Beijing 100083, China

* Correspondence: ning.yuan@cumtb.edu.cn

Abstract: Recently, controlled low-strength material (CLSM) has been considered an easy-to-mix material, and the raw material is usually derived from solid waste, suggesting lower production costs. Moreover, the resource utilization of waste fosters the sustainable advancement of both society and the environment. In the present work, a CLSM with excellent performance was developed by adopting fly ash, bottom ash, desulfuration gypsum, and cement as the main cementitious materials, as well as gasification coarse slag and coal gangue as aggregates. An orthogonal experiment with three factors and three levels was designed according to the ratio of cement to binder, the contents of water, and the water-reducing agent. Further, the macroscopic properties of flowability, dry density, bleeding, compressive strength, fresh density, porosity, and absorption rate of the CLSM mixtures were tested. To optimize the CLSM proportion, the ranges of three indicators of CLSM were calculated. Experimental results manifested that the fresh and dry densities of the mixtures were within the range recommended by ACI 229. The optimal levels of cement–binder ratio (i.e., the ratio of cement to binder), water content, and water-reducing agent content are 0.24, 248 kg·m⁻³, and 0.80 kg·m⁻³, respectively. Under this condition, the flowability was 251 mm, the bleeding was 3.96%, and the compressive strength for 3 d, 7 d, and 28 d was 1.50 MPa, 3.06 MPa, and 7.79 MPa, respectively. Furthermore, the leaching values of eight heavy metals in CLSM and raw materials were less than the standard requirements, indicative of no leaching risk.



Citation: Chen, T.; Yuan, N.; Wang, S.; Zhang, X.; Lin, C.; Wu, X.; Wang, Q.; Wang, D. Optimization of Controlled Low-Strength Material from Multi-Component Coal-Based Solid Waste. *Sustainability* **2024**, *16*, 1513. <https://doi.org/10.3390/su16041513>

Academic Editor: Paolo S. Calabrò

Received: 22 December 2023

Revised: 27 January 2024

Accepted: 7 February 2024

Published: 10 February 2024



Copyright: © 2024 by the authors. Licensee MDPI, Basel, Switzerland. This article is an open access article distributed under the terms and conditions of the Creative Commons Attribution (CC BY) license (<https://creativecommons.org/licenses/by/4.0/>).

Keywords: controlled low-strength material; coal industry by-product; orthogonal experiment; range analysis; heavy metal leaching

1. Introduction

The American Concrete Institute (ACI) 229 Committee has defined controlled low-strength material (CLSM) as a self-compacting cementing material that originally served as a structural fill or backfill [1,2]. The CLSM is fluid and easy to mix and can penetrate confined spaces that are difficult for compact devices to reach. In addition, CLSM cures quickly, thus avoiding the need for long construction cycles [3]. Therefore, CLSM is a multifunctional backfilling material and can be useful for groove backfilling [4], ground heat exchangers [5], urban pipeline buffering [6], underground space backfilling [7] (such as goaf and abandoned underground tunnels), roadbed [8], abutment back [9], and erosion prevention slope filling [10]. CLSM is eco-friendly, low-budget, and low labor intensive. At the initial stage of pouring, CLSM has high ductility and shows similar characteristics to the soil. But with age, CLSM will emerge with high strength and low ductility like concrete [9]. Most of the knowledge and literature on the application of CLSM has been associated with the application of concrete material engineering and geotechnical engineering, but neither of these fields has caused extensive concern. Besides, in the application of CLSM, its applicability ought to be strictly estimated according to the engineering application; the capability of CLSM can be boosted by regulating the material composition of CLSM.

In the past few decades, China has produced a mass of coal-based solid waste in the process of coal production and utilization, and the resultant waste includes coal gangue, fly ash, bottom ash, gasification slag, and desulfurization gypsum [11]. Their stacking occupies large amounts of land, leading to serious pollution of the surrounding environment, such as the atmosphere, water, soil, etc., and then contributing harm to humans and animals [12,13]. Comprehensive utilization of resources is an important part of China's sustainable development strategy. Promoting the utilization of solid waste is of great significance for improving environmental quality and promoting sustainable social development [14]. Based on its requirement of achieving lower strength, CLSM can be produced by solid waste as its cementitious material or aggregate [15,16]. As a consequence, coal-based solid waste can be utilized to substitute the cementitious materials and aggregates of CLSM, reducing the stacking of coal-based solid waste and reducing the pollution to the surrounding environment [17,18]. For instance, Cheng et al. used bottom ash instead of fly ash to study the effect of the ratio of fly ash to bottom ash on the filling material. Experimental results showed that magnifying the ratio of fly ash to bottom ash enhanced the performance of the material, like slump, setting time, and mechanical strength [19]. Additionally, Wang et al. conducted a filling experiment using coal gangue as aggregate and verified the filling effect using a dynamic filling simulation device. The results showed that the prepared CLSM could meet the requirements of filling design and application [7]. Consequently, the development of CLSM using coal-based solid waste has significant economic and environmental benefits. Besides, other solid waste has also been used to make CLSM. Kuo et al. replaced cement with 20% fly ash and used broken oyster shells as aggregate (particle size close to that of natural fine aggregate). The results showed that the compressive strength was not significantly reduced when 20% oyster shells were added instead of sand, indicating that the reasonable application of oyster shells was feasible in CLSM [20]. Zhen et al. prepared CLSM using dewatered sludge and refuse incineration (MSWI) bottom ash. The mechanical properties, microstructure, and leaching of harmful substances (organic substances) of CLSM were studied. Among them, the portion larger than 40 mm was removed after MSWI screening and then heat treated at 900 °C. The results showed that the addition of MSWI bottom ash improved the compressive strength of the CLSM sample, and the leachable substances exerted no harm on health and the environment [21]. Other solid waste for the preparation of CLSM includes soft shale from coal mine overburden [22], dimension stone sludge [23], cement kiln dust [24], waterworks sludge [25], waste glass powder [26], etc.

The components in CLSM interact with each other, and changes in component content can affect the final properties of CLSM, such as flowability, bleeding, and compressive strength [27]. The dosage of a certain material cannot be adjusted independently without affecting the mixing ratio, so its mixing ratio is generally obtained by changing the ratio recommended in ACI 229R by trial and error [1]. The experimental design of this trial-and-error method has contingency and limitations, while the orthogonal experimental design can explain the influence of different experimental factors alone or synergistically through fewer experiments, which greatly reduces the experimental workload and improves the work efficiency [23]. For instance, Wang and colleagues explored the optimum ratio of the filler material with fly ash, desulfurization gypsum, and coal gangue as the main components through orthogonal experiments and found that the content of the cementitious material mainly composed of fly ash was the primary factor affecting the strength [7]. Furthermore, Lan et al. prepared CLSM with copper slag produced by copper smelting as the main raw material and used orthogonal experiments to determine the effects of three chemical activators (lime, NaOH, and triethanolamine) and grinding time on the properties and structure of copper slag-based CLSM. The optimum ratio of CLSM to satisfy the filling performance was obtained [28]. Chen et al. selected four controllable factors, used the Taguchi method, and adopted the L9(3⁴) orthogonal arrangement to optimize the conditions for CLSM production using dimension stone sludge. The results indicated that the amount of stone sludge had the most important impact on the compressive strength, and the best mix ratio of using stone sludge to produce CLSM was obtained [23]. Therefore,

previous studies have shown the feasibility of orthogonal experimental design and the superiority of determining the best CLSM ratio.

Currently, the utilization of multicomponent coal-based solid waste to prepare CLSM has been rarely studied, especially on the impact of heavy metal ion leaching of CLSM on the environment. Inspired by the above literature results, we adopted five kinds of coal industrial solid waste, including fly ash, desulfurization gypsum, bottom ash, gasification slag as well as coal gangue, and a handful of cement as raw materials for developing a CLSM. By using the orthogonal experiment to optimize the experimental plan, nine kinds of mixtures were prepared. The effects of three factors (cement–binder ratio (i.e., the ratio of cement to binder), water content, and water-reducing agent content) on the flowability, bleeding, and compressive strength of CLSM were studied. Through the range analysis method, the sensitivity of each factor to the performance was compared and analyzed, and the best CLSM mix ratio was finally obtained. Additionally, the fresh density, dry density, porosity, and absorption rate of the nine mixtures were investigated. Furthermore, scanning electron microscopy (SEM) and heavy metal ion leaching analysis were carried out on the CLSM products to evaluate the microstructures and environmental effects.

2. Experimental Programs

2.1. Materials and Methods

P. I 42.5 Portland cement was used in this work. The water-reducing agent was a powdered polycarboxylate superplasticizer (Sika 540P) produced by Shanghai Chenqi Chemical Technology Co., Ltd. In addition, bottom ash, fly ash, and desulfurization gypsum were from Yuanyang Lake Power Plant in Ningxia, China, where the bottom ash was ball milled by a ball mill for 20 min. The coal gangue, crushed by a two-stage jaw crusher, was from the Renjiazhuang coal mine in Ningxia. The gasification coarse slag was also from the Ningxia coal mine. Their compositions are tabulated in Table 1, and the particle size distributions are shown in Figure 1.

Table 1. Chemical compositions of cement and coal-based solid wastes (wt%).

Raw Materials	Composition (%)	SiO ₂	Al ₂ O ₃	CaO	Fe ₂ O ₃	MgO	Na ₂ O	K ₂ O	TiO ₂	SO ₃	f-CaO	Cl ⁻	Loss
	Cement		20.72	4.62	62.18	3.26	3.15	0.52	0.34	–	2.72	0.72	0.012
Fly ash		52.95	27.55	4.94	6.31	1.92	1.52	1.85	1.28	1.03	–	–	0.19
Bottom ash		56.37	26.71	3.41	6.62	1.2	1.08	1.58	1.04	0.47	–	–	1.09
Desulfurization gypsum		2.62	0.58	28.77	0.43	2.46	0.25	0.12	0.03	40.17	–	–	24.5
Coal gangue		48.46	24.13	0.1	9.44	0.47	0.25	1.99	0.86	0.09	–	–	14.03
Gasification slag		48.07	16.37	8.95	8.84	1.91	1.77	1.48	0.9	0.61	–	–	10.3

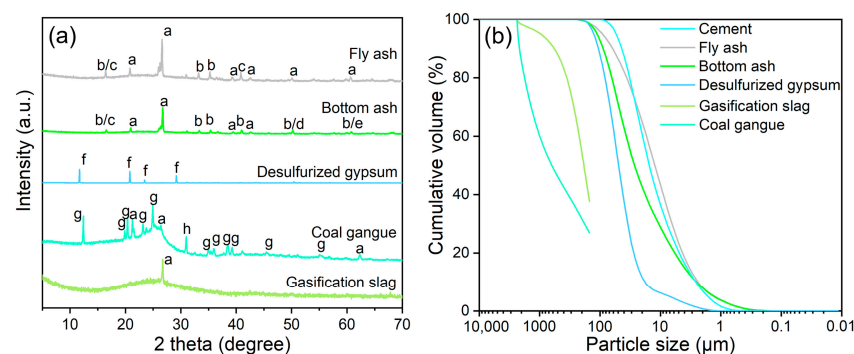


Figure 1. (a) XRD patterns of fly ash, bottom ash, desulfurization gypsum, coal gangue, and gasification slag. Components: a-SiO₂, b-3Al₂O₃·2SiO₂, c-Al₂[SiO₄]O, d-Fe₂O₃, e-CaO, f-CaSO₄(H₂O)₂, g-Al₂Si₂O₅(OH)₄, h-FeS₂. (b) Particle size distributions of cement, fly ash, bottom ash, desulfurization gypsum, gasification slag, and coal gangue.

All raw materials were adopted after natural drying at room temperature, and CLSM was prepared according to the experimental scheme and mixing procedure. A mold of 70.7 mm × 70.7 mm × 70.7 mm was used. After 36 h, the samples were demolded and put into a curing box for curing (SHBY-40B, Cangzhou Huaxi, humidity above 95%, temperature 20 ± 1 °C) for 3 d, 7 d, and 28 d, and then the performance test was carried out. CLSM mixing procedures, flowability (ASTM D6103-17 [29]), bleeding (GB/T 50080-2016 [30]), fresh density (GB/T 50080-2016 [30]), dry density (ASTM D6023-2016 [31]), porosity (ASTM D6023-2016 [31]), absorption (ASTM D6023-2016 [31]), compressive strength (GB/T 50081-2019 [32]), and metal leaching test procedures (HJ 557-2010 [33]) were tested according to their respective standards. The details are shown in Supplementary Materials (Pages S2–S4). In addition, SEM and laser particle size analysis test details are also available in Supplementary Materials (Page S2).

2.2. Experimental Design and Data Analysis

Three factors [23,27] (cement–binder ratio, water content, and water-reducing agent content) that have the greatest impact on the three indicators of CLSM flowability, bleeding, and compressive strength were selected, and three levels were set for each factor, as displayed in Table 2. In order to reduce the workload, the Taguchi method was employed to optimize the test plan [23,34], and the L9 (3^3) orthogonal arrangement was used (Table 3).

Table 2. Factors and levels of orthogonal experiments of CLSM preparation.

Factor	Cement–Binder Ratio (A)	Water Content ($\text{kg}\cdot\text{m}^{-3}$) (B)	Water-Reducing Agent Content ($\text{kg}\cdot\text{m}^{-3}$) (C)
Level 1	0.16	248	0.64
Level 2	0.24	272	0.80
Level 3	0.32	296	0.96

Table 3. Orthogonal experimental arrangement of L9(3^3).

No.	Cement–Binder Ratio (A)	Water Content ($\text{kg}\cdot\text{m}^{-3}$) (B)	Water-Reducing Agent Content ($\text{kg}\cdot\text{m}^{-3}$) (C)
1	1 (0.16)	1 (248)	1 (0.64)
2	1 (0.16)	2 (272)	2 (0.80)
3	1 (0.16)	3 (296)	3 (0.96)
4	2 (0.24)	1 (248)	2 (0.80)
5	2 (0.24)	2 (272)	3 (0.96)
6	2 (0.24)	3 (296)	1 (0.64)
7	3 (0.32)	1 (248)	3 (0.96)
8	3 (0.32)	2 (272)	1 (0.64)
9	3 (0.32)	3 (296)	2 (0.80)

The range analysis method possesses the merits of simple calculation, easy understanding, and intuitive results. It is the most common method of analysis in orthogonal experiments. The maximum value minus the minimum value of the data represents the range, which is on behalf of the amount of variation in the data [35]. The degree of influence of different experimental factors on the indicators under investigation can be quantitatively described by the results of range analysis. This experiment discusses the connection between CLSM and various influencing factors. Specifically, it includes calculating the range of all factors, obtaining the optimal combination of the importance ranking and matching the ratio of different influencing factors, and drawing the trend graph of each influencing factor and indicator.

2.3. Mixture Proportions

In the experiment, fly ash, desulfuration gypsum, bottom ash, coal gangue, gasification slag, and cement were used as raw materials to obtain CLSM. The specific ratio is given according to the preliminary work of the experiment. The ratio of cementitious material to aggregate was fixed at 0.33. The amounts of coal gangue, gasification slag, desulfuration

gypsum, and bottom ash remained unchanged, accounting for 60%, 15%, 3%, and 5% of the solid material, respectively. Fly ash was used to substitute cement when the ratio of cement to binder was changed. The details are provided in Table 4.

Table 4. The specific experimental scheme of CLSM orthogonal test.

No.	Aggregate ($\text{kg}\cdot\text{m}^{-3}$)		Cementitious Materials ($\text{kg}\cdot\text{m}^{-3}$)				Water ($\text{kg}\cdot\text{m}^{-3}$)	Water-Reducing Agent ($\text{kg}\cdot\text{m}^{-3}$)
	Coal Gangue	Gasification Slag	Cement	Fly Ash	Bottom Ash	Desulfurized Gypsum		
1	960	240	64	208	80	48	248	0.64
2	960	240	64	208	80	48	272	0.80
3	960	240	64	208	80	48	296	0.96
4	960	240	96	176	80	48	248	0.80
5	960	240	96	176	80	48	272	0.96
6	960	240	96	176	80	48	296	0.64
7	960	240	128	144	80	48	248	0.96
8	960	240	128	144	80	48	272	0.64
9	960	240	128	144	80	48	296	0.80

3. Results and Discussion

The flowability, bleeding, fresh density, dry density, compressive strength (3 d, 7 d, and 28 d), porosity, and absorption rate of nine CLSM were investigated in this work, as shown in Table 5. Figure 2 also gives an intuitive plot of porosity, absorption rate, fresh density, and dry density. Notably, both fresh and dry densities are within the normal CLSM range reported by ACI Committee 229 (i.e., fresh density between $1842 \text{ kg}\cdot\text{m}^{-3}$ and $2323 \text{ kg}\cdot\text{m}^{-3}$ and dry density between $1762 \text{ kg}\cdot\text{m}^{-3}$ and $1890 \text{ kg}\cdot\text{m}^{-3}$) [1].

Table 5. Various test result data for nine CLSM mixtures.

No.	Flowability (mm)	Bleeding (%)	Compressive Strength (MPa)			Porosity (%)	Absorption (%)	Fresh Density ($\text{kg}\cdot\text{m}^{-3}$)	Dry Density ($\text{kg}\cdot\text{m}^{-3}$)
			3 d	7 d	28 d				
1	150	2.49	1.02	2.42	3.63	13.78	15.98	1985	1778
2	320	5.67	0.84	2.31	3.14	14.12	16.44	2015	1782
3	350	5.25	0.74	1.86	2.46	13.26	15.29	2093	1859
4	251	3.96	1.50	3.06	7.79	13.27	15.30	2023	1810
5	350	11.00	1.33	2.87	7.29	13.75	15.94	2047	1812
6	260	9.43	0.99	2.36	6.24	14.41	16.83	2019	1778
7	270	2.13	2.15	3.49	13.95	12.69	14.53	2075	1849
8	255	4.76	1.73	2.98	11.97	13.15	15.14	2084	1847
9	315	13.73	1.49	2.71	11.12	13.99	16.26	2031	1786

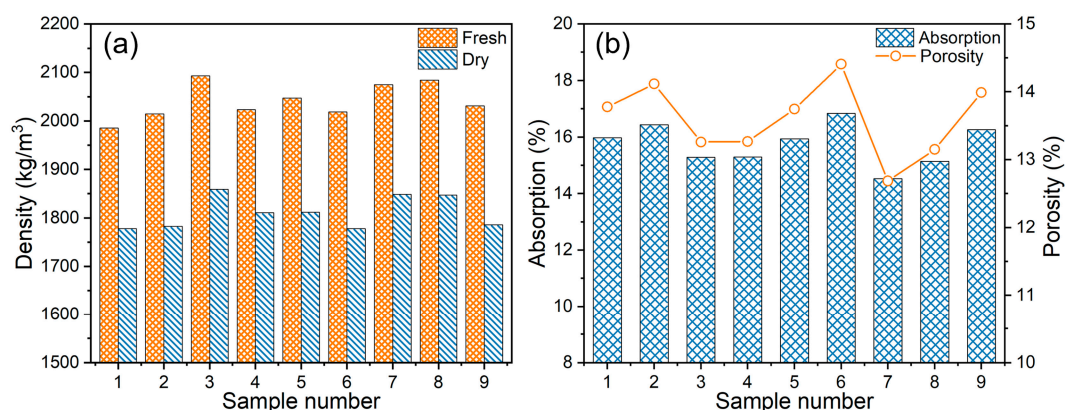


Figure 2. Test results of the prepared CLSM mixtures. (a) Fresh density and dry density, (b) absorption and porosity.

3.1. Flowability

Flowability indicates the workability performance of CLSM [1]. In general, CLSM blends with high moisture content have good flow properties. However, adding a large amount of water to CLSM may lead to increased bleeding, decreased strength, and even

aggregate segregation. Therefore, to obtain the best engineering performance of CLSM, it is necessary to carry out a reasonable optimization design of the mix ratio.

The flowability test results for all CLSM mixtures are displayed in Figure 3. The flowability varies in the range of 150–300 mm, all conforming to the high flowability grade with the exception of group 1 [1].

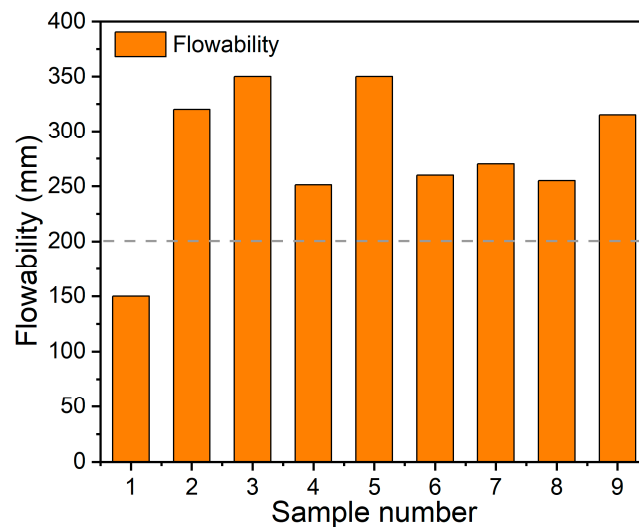


Figure 3. Flowability results of various CLSM.

3.1.1. Single Factor Analysis

Figure 4 summarizes the influence laws of the designed influencing factors on flowability. Figure 4a exhibits the effect of the cement–binder ratio on the flowability of CLSM. As shown in the figure, the flowability of the CLSM mixtures fluctuates in the range of 273–287 mm. When increasing the cement–binder ratio, the overall trend of the flowability of the CLSM increases first and then decreases.

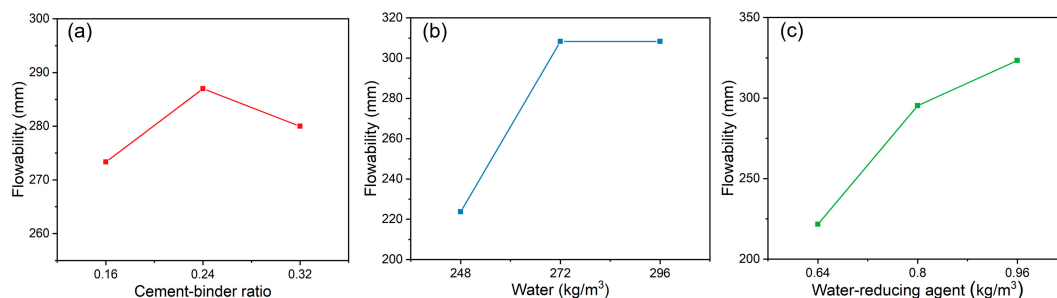


Figure 4. Effects of single factor analysis on flowability properties of CLSM: (a) cement–binder ratio; (b) water content; (c) water-reducing agent content.

With the cement–binder ratio of 0.16, the flowability is 273 mm, indicating that the slurry possesses good flowability. When the cement–binder ratio changes from 0.16 to 0.24, the flowability increases by 14 mm and the flowability of the CLSM increases to a maximum value of 287 mm. This is because when the cement–binder ratio is 0.16 to 0.24, the water content can meet the wetting of the cementing material, and the flowability increases. When amplifying the cement–binder ratio, the flowability of the mixed slurry decreases. This is due to the further increase in cement content; the small cement particles require more water to moisten, and the lack of water content leads to reduced flowability. In addition, when the cement–binder ratio is 0.32, the flowability of the mixed slurry reaches 280 mm.

Figure 4b presents the relationship between water content and CLSM flowability. When increasing in water content, the flowability first increases and then remains unchanged. The water content increases from 248 kg·m^{−3} to 272 kg·m^{−3}, and the flowability

increases significantly from 224 mm to 308 mm. This is because when water content increases, the packing density of solid particles in the slurry decreases, the distance between adjacent particles widens, the number of direct contacts between particles decreases, and thus, the flow performance increases. When the water content increases to $296 \text{ kg}\cdot\text{m}^{-3}$, the flowability does not climb with the water content. Under this condition, the flowability has reached the maximum value, and increasing the amount of water will not enhance the flowability, but will lead to segregation and serious bleeding of the CLSM mixtures.

Figure 4c presents the relationship between the content of water-reducing agent content and the flowability of CLSM. As presented in the figure, the flowability of CLSM is positively correlated with the amount of water-reducing agent added, and the flowability of the CLSM mixture fluctuates in the range of 222–323 mm. When increasing the amount of water-reducing agents, the flowability shows a gradual upward trend. This is due to the disintegration of the flocculated particles in the presence of the water-reducing agent, and the encapsulated water is released, thereby effectively enhancing the flowability of the CLSM mixtures [36].

3.1.2. Range Analysis

Table 6 displays the experimental range analysis results of the flowability experiment of the CLSM mixtures. From the table, the content of the water-reducing agent is the most critical factor affecting the change of flowability, followed by the content of the water, and the ratio of cement to binder has the least effect.

Table 6. Range analysis results of flowability in the orthogonal test of CLSM.

Performance Parameter	Experimental Control Factor	Cement–Binder Ratio (A)	Water Content ($\text{kg}\cdot\text{m}^{-3}$) (B)	Water-Reducing Agent Content ($\text{kg}\cdot\text{m}^{-3}$) (C)	Rank
Flowability (mm)	Level 1	273	224	222	C > B > A
	Level 2	287	308	295	
	Level 3	280	308	323	
	Range analysis	14	84	101	

3.2. Bleeding

The bleeding of CLSM represents its degree of settlement. It is defined as the volume of exuded water as a percentage of the initial mixing water volume of the fresh CLSM mixture. Usually, CLSM with high water content is more likely to secrete more water, and water-reducing agents can reduce the amount of water used in CLSM so that CLSM can secrete less water; this meets the standard requirements. Therefore, the influence of various factors must be comprehensively considered in order to obtain good CLSM products. From Figure 5, for CLSM mixtures, the bleeding fluctuated greatly, ranging from 2.03% to 13.3%. A lower bleeding value prevents volumetric expansion, which can form gaps. Therefore, CLSM must have a low bleeding value, and the acceptable limit for bleeding is 5% [1].

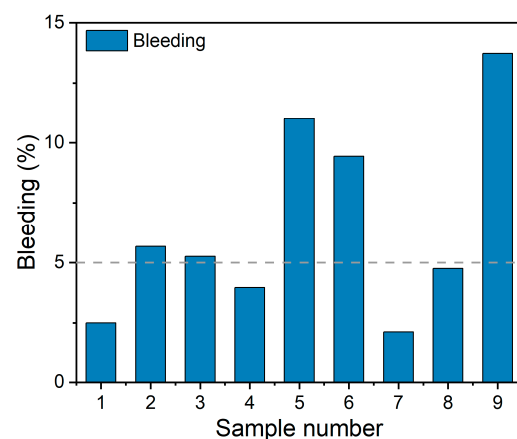


Figure 5. Bleeding of various CLSM mixtures.

3.2.1. Single Factor Analysis

The influence of these three influencing factors on bleeding is presented in Figure 6. Figure 6a illustrates the regularity of the influence of the cement–binder ratio on the bleeding of CLSM. The average bleeding of CLSM materials fluctuates in the range of 4.47–8.10%. When the ratio of cement to binder in the CLSM mixture is increased, the bleeding displays a trend of first growing and then declining. When the cement–binder ratio is 0.16, the bleeding is 4.47%, which meets the requirement of less than 5% bleeding. When the cement–binder ratio increases from 0.16 to 0.24, the bleeding increases. Then, increasing the cement–binder ratio from 0.24 to 0.32 decreases the bleeding, which may be attributed to the high consumption of water during cement hydration, resulting in less free water available for bleeding [37]. Figure 6b expresses the relationship curve between the amount of water added and the bleeding rate of CLSM. From Figure 6b, the water content increases from $248 \text{ kg}\cdot\text{m}^{-3}$ to $272 \text{ kg}\cdot\text{m}^{-3}$, and the bleeding of the CLSM increases from 2.2% to 9.47%, manifesting a significant increase. The bleeding of CLSM increases linearly with the addition of water. This is because a higher water–cement ratio can lead to more free water in the CLSM slurry, which will be easy to bleed. Figure 6c presents the relationship between the content of the water-reducing agent and CLSM bleeding. As exhibited in Figure 6c, the average bleeding of CLSM fluctuates in the range of 5.56–7.78%, and the fluctuation range is small. However, due to its small dosage, it has no significant effect on the overall bleeding of CLSM.

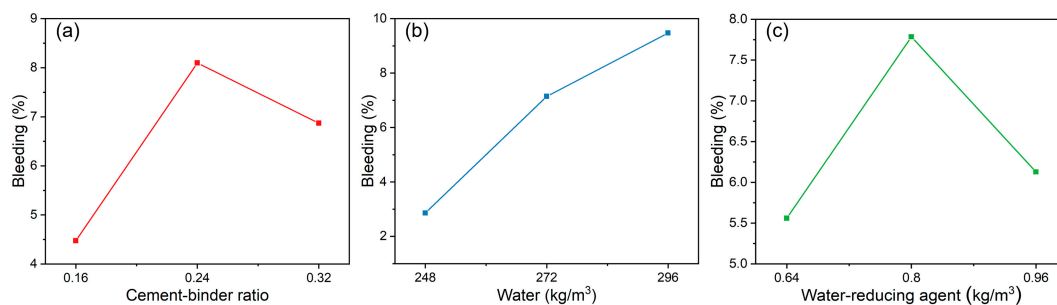


Figure 6. Effects of single factors on bleeding of CLSM: (a) cement–binder ratio; (b) water content; (c) water-reducing agent content.

3.2.2. Range Analysis

The range analysis was conducted on the results of the CLSM bleeding experiment, and the analysis results are listed in Table 7. As shown in the table, the content of water can significantly affect the change of CLSM bleeding, followed by the ratio of cement to binder, and the content of the water-reducing agent is the least influencing factor.

Table 7. Range analysis results of bleeding in the orthogonal test of CLSM.

Performance Parameter	Experimental Control Factor	Cement–Binder Ratio (A)	Water Content ($\text{kg}\cdot\text{m}^{-3}$) (B)	Water-Reducing Agent Content ($\text{kg}\cdot\text{m}^{-3}$) (C)	Rank
Bleeding	Level 1	4.47	2.86	5.56	B > A > C
	Level 2	8.10	7.14	7.78	
	Level 3	6.87	9.47	6.13	
	Range analysis	3.63	6.61	2.22	

3.3. Compressive Strength

Compressive strength is a measure of the load-carrying capacity of a CLSM. The amount of cement and water are the most important factors determining the strength of CLSM. The greater the ratio of water content to cement content, the greater the number of pores in CLSM, the smaller the bonding force with aggregate, and the lower the strength of

CLSM. On the contrary, the CLSM compressive strength will be higher when the cement content increases or the water content decreases.

The compressive strength test results of the CLSM mixtures at 3 d, 7 d, and 28 d ages are displayed in Figure 7a–c. The compressive strength of all CLSM increases with curing age. The compressive strength ranges from 0.84 to 2.15 MPa at 3 d age, 1.84–3.49 MPa at 7 d age, and 2.49–13.95 MPa at 28 d age, respectively. Applications such as structural filling require the CLSM to have sufficient load capacity. As time passes, the compressive strength of CLSM becomes higher, making future excavation difficult. Removability modulus (RE) can be used to evaluate the excavability of CLSM based on their compressive strength and dry density [37,38].

$$RE = \frac{0.619 \times W^{1.5} \times C^{0.5}}{10^6} \quad (1)$$

where W is the dry density of the CLSM in ($\text{kg}\cdot\text{m}^{-3}$) and C is the compressive strength at 28 d in (kPa).

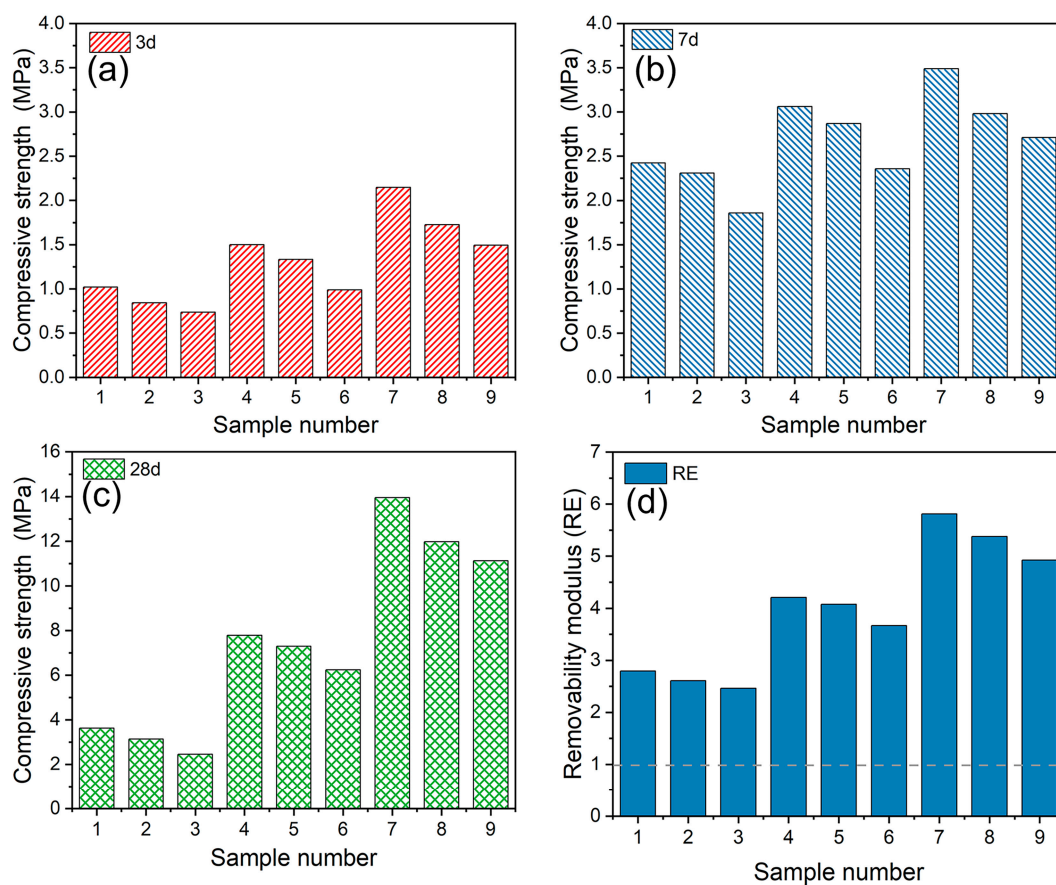


Figure 7. Results of (a) 3 d, (b) 7 d, (c) 28 d CLSM compressive strength, and (d) removability modulus.

If the RE is less than 1, the CLSM is considered to be easy to remove. The RE values for all tested CLSM mixtures are presented in Figure 7d. The RE values of all samples are higher than 1. Hence, mining these CLSM mixtures by hand is difficult. These CLSM mixtures can be applied to projects that do not require excavation at a later stage.

3.3.1. Single Factor Analysis

Figure 8 shows the effects of three factors on the compressive strength of CLSM at different curing ages (3 d, 7 d, and 28 d). According to Figure 8, the compressive strength of CLSM gradually increases when increasing the cement–binder ratio. This result can be ascribed to the increase in cement content; the pozzolanic reaction rate between fly

ash, silicate in bottom ash, and CH (calcium hydroxide) becomes faster, and more C-S-H (calcium silicate hydrate) is formed [39,40]. Therefore, the CLSM mixture with a cement–binder ratio of 0.32 has the highest strength. In the next part, the compressive strength of all CLSM decreases gradually as the water content increases from $248 \text{ kg}\cdot\text{m}^{-3}$ to $272 \text{ kg}\cdot\text{m}^{-3}$. This is due to the increase in water content, which increases the free water in the CLSM [41]. The excess water causes the CLSM to form pores after hardening, which greatly reduces its actual effective cross-section for resisting loads [42]. Hence, the compressive strength decreases with the water content. Furthermore, the additional amount of water-reducing agent has little effect on the compressive strength of CLSM at three ages.

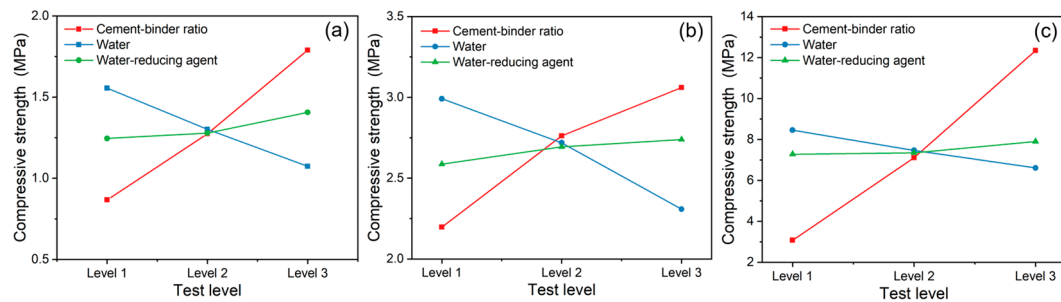


Figure 8. Effect of single factors on 3 d (a), 7 d (b), and 28 d (c) compressive strength of CLSM.

3.3.2. Range Analysis

Table 8 shows the range analysis results of the compressive strength experiments of CLSM. From the table, the ratio of cement to binder is the most important factor influencing the change of compressive strength of CLSM, followed by the content of water, and the content of the water-reducing agent has the least effect. It is illustrated that for the strength development of the hardened body of the CLSM mixture, the cement contributes the most, but since the upper limit of the strength of CLSM is 8.3 MPa, the second level is the most suitable.

Table 8. Range analysis results of compressive strength in the orthogonal test of CLSM.

Performance Parameter	Experimental Control Factor	Cement–Binder Ratio (A)	Water Content ($\text{kg}\cdot\text{m}^{-3}$) (B)	Water-Reducing Agent Content ($\text{kg}\cdot\text{m}^{-3}$) (C)	Rank
3 d	Level 1	0.87	1.56	1.25	A > B > C
	Level 2	1.27	1.30	1.28	
	Level 3	1.79	1.07	1.41	
	Range analysis	0.92	0.49	0.16	
7 d	Level 1	2.20	2.99	2.59	
	Level 2	2.76	2.72	2.69	
	Level 3	3.06	2.31	2.74	
	Range analysis	0.86	0.68	0.15	
28 d	Level 1	3.08	8.45	7.28	
	Level 2	7.11	7.47	7.35	
	Level 3	12.34	6.61	7.90	
	Range analysis	9.26	1.84	0.62	

3.4. Determination of Optimal Sample and Microscopic Analysis

Based on the above analysis, the optimal sample combination is determined. The first is factor A (cement–binder ratio), whose flowability belongs to the category of high flowability, and bleeding is at the edge of 5%. A is the main factor affecting the compressive strength, so level 2 (0.24) should be selected according to the compressive strength level (the compressive strength of 28 d should be greater than 3 MPa and less than 8.3 MPa) [43].

The second factor is factor B (water content), which belongs to the high flowability category, and the bleeding is less than 5% when the bleeding level is 1. B is the main factor

affecting the bleeding level, and the compressive strength (28 d) is at the edge of 8.3 MPa. Therefore, the optimal level ought to be selected according to the bleeding level, and level 1 ($248 \text{ kg}\cdot\text{m}^{-3}$) should be selected.

The final factor is the selection of factor C (water-reducing agent content). The flowability belongs to the high flowability category, the bleeding is more than 5%, and the strength meets the standard requirements. The water-reducing agent has the most significant influence on the flowability. According to the range analysis and experimental results, level 2 and level 3 should be selected. In consideration of the cost, level 2 (0.80) should be chosen. Therefore, the optimal combination is A (0.24), B (248), and C (0.80), that is A2B1C2.

By means of orthogonal optimization experiments and range analysis, the optimal levels of cement–binder ratio, water content, and water-reducing agent dosage were obtained as 0.24, $248 \text{ kg}\cdot\text{m}^{-3}$, and $0.80 \text{ kg}\cdot\text{m}^{-3}$, respectively. In conclusion, this optimal combination appears in the orthogonal experiment (the fourth group), and its flowability is 251 mm, bleeding is 3.96%, and compressive strength (28 d) is 7.79 MPa, all of which meet the requirements of filling.

The optimal samples at 3, 7, and 28 d of age were selected for the SEM test (Figure 9). The results manifest that the unreacted spherical fly ash particles are observed in the microstructure of all samples. The presence of this result is ascribed to the high silica content in the system. C-S-H gel, ettringite, microcracks, and micropores can be observed. In addition, the content of ettringite and C-S-H gel in 28 d samples is much higher than that in 3d and 7d samples, which is due to the gradual deepening of the hydration reaction of each raw material with the extension of curing age.

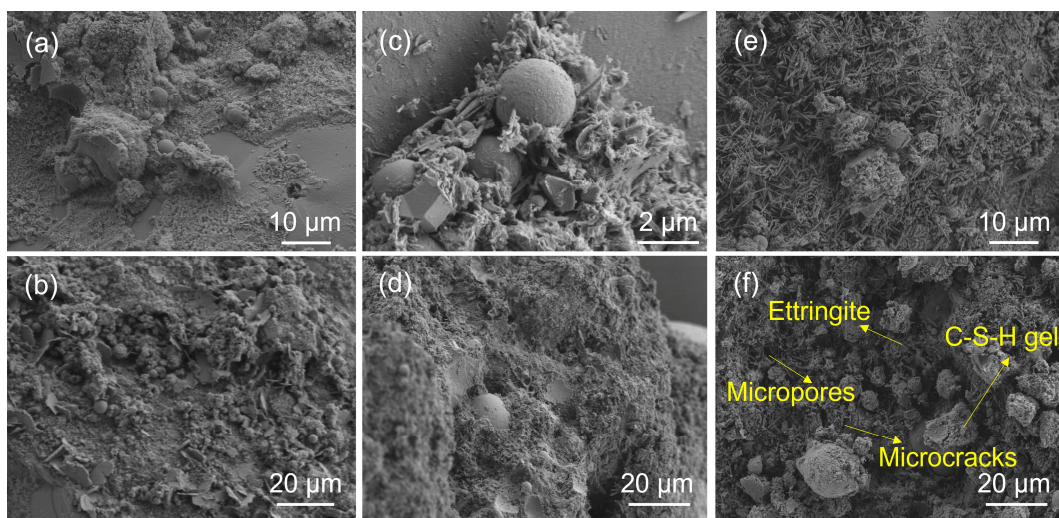


Figure 9. SEM images of optimal CLSM samples at 3 d (a,b), 7 d (c,d), and 28 d (e,f).

3.5. Leaching of Heavy Metals

When coal-based solid waste is employed to prepare CLSM for underground filling, the main environmental problem is that dangerous chemical elements may seep into groundwater at certain concentrations, thus endangering human health and the natural environment. For this purpose, the environment under which the samples were leached by surface water or groundwater was simulated to detect the leaching risk of inorganic pollutants from solid waste. The optimal CLSM samples and five coal-based solid wastes were tested for heavy metals leaching. As CLSM is expected to be applied for underground filling in coal mines, experiments are carried out by referring to China's national environmental protection standard HJ 557-2010 and using experimental methods within the standard range [33]. GB 5085.3-2007 was adopted to check whether the leaching of CLSM heavy metals exceeded the permissible range [44]. In this work, eight metallic elements were selected, namely Cr, Mn, Cu, Zn, As, Cd, Pb, and Hg.

At the same time, Table 9 lists the metal leaching results. The heavy metal leaching content of raw materials and CLSM mixture is lower than the value specified in the standard [44], so it can be determined that raw materials and CLSM mixture have no leaching toxicity. This is conducive to the application of CLSM products and has a positive effect on the sustainable development of the environment.

Table 9. Leaching of heavy metal elements from raw materials and optimal CLSM ($\mu\text{g}\cdot\text{L}^{-1}$).

Heavy Metal	Cr	Mn	Cu	Zn	As	Pb	Cd	Hg
Gasification slag	494.60	5.42	3.88	59.13	3.07	11.56	0.75	5.38
Coal gangue	0.00	635.24	0.55	141.77	0.09	0.07	0.33	0.05
Fly ash	727.81	1.79	1.96	30.64	3.18	11.90	4.33	1.45
Desulfurized gypsum	0.23	138.55	4.66	6.41	5.97	0.04	0.83	0.11
Bottom ash	3.40	0.22	0.02	7.85	3.09	0.02	0.00	0.24
Optimal sample	79.61	1.07	8.61	37.15	0.40	9.87	0.58	2.22
GB 5085.3-2007	5000	-	100,000	100,000	5000	5000	1000	100

There are two possible reasons for the change of metal ion leaching content in CLSM samples: (1) The material in CLSM forms C-S-H gel due to hydration, and heavy metal ions are physically adsorbed or wrapped by the gel, which promotes the solidification of heavy metal ions [45]. (2) Heavy metals are involved in the reaction, and heavy metals such as Cr, Cu, and Pb replace calcium in C-S-H gel or heavy metal hydroxide may replace CH. Therefore, the leaching content of heavy metals was reduced [46].

4. Conclusions

This study is primarily concerned with the optimization of the preparation and performance of CLSM based on five coal industry by-products (fly ash, desulfurization gypsum, bottom ash, gasification slag, as well as coal gangue). The macroscopic properties of CLSM like flowability, bleeding, compressive strength, fresh density, dry density, absorption rate, and porosity, were studied. The effects of the cement–binder ratio, water content, and water-reducing agent content on the property indexes (flowability, bleeding as well as compressive strength) of the prepared CLSM were investigated. The micromorphology of CLSM products and the leaching risk of heavy metal ions from solid waste were explored. A usable CLSM product has been obtained, which will promote the utilization of solid waste and contribute to the goal of sustainable development of society. The main conclusions can be summarized as follows:

- (1) The fresh and dry densities of CLSM are within the range recommended by ACI 229.
- (2) For the bleeding and flowability of CLSM, the water content has the greatest influence, whereas the cement–binder ratio has the most significant effect on the compressive strength of CLSM.
- (3) As the cement–binder ratio increases, the flowability first decreases and then increases, the bleeding increases first and then decreases, and the compressive strength increases uniformly. When the water content increases, the flowability and bleeding increase all the time, but the compressive strength shows an opposite trend. When the content of the water-reducing agent increases, the flowability increases greatly, the bleeding increases first and then decreases, the compressive strength increases slightly, and the effect on the compressive strength is inconspicuous.
- (4) By means of orthogonal optimization experiments and range analysis, the optimal levels of cemen–binder ratio, water content, and water-reducing agent dosage were obtained as 0.24, 248 $\text{kg}\cdot\text{m}^{-3}$, and 0.80 $\text{kg}\cdot\text{m}^{-3}$, respectively. Hereon, the flowability was 251 mm, the bleeding was 3.96%, and the compressive strength for 3 d, 7 d, and 28 d was 1.50 MPa, 3.06 MPa, and 7.79 MPa, respectively.
- (5) The leaching values of the prepared CLSM optimal sample and the eight heavy metal elements (Cr, Mn, Cu, Zn, As, Cd, Pb, and Hg) in the raw materials are far lower

than the safety limits in the standard, indicating that the CLSM has no heavy metal leaching risk and has limited influence on the environment.

Supplementary Materials: The following supporting information can be downloaded at <https://www.mdpi.com/article/10.3390/su16041513/s1>.

Author Contributions: Conceptualization, N.Y., T.C. and S.W.; Data curation, T.C., N.Y. and S.W.; Formal analysis, T.C., S.W., X.Z., C.L. and X.W.; Funding acquisition, N.Y.; Investigation, T.C., S.W., C.L. and X.W.; Methodology, T.C., N.Y. and S.W.; Project administration, N.Y.; Resources, N.Y., Q.W. and D.W.; Supervision, N.Y.; Validation, T.C., N.Y., S.W. and C.L.; Visualization, T.C., N.Y. and S.W.; Writing—original draft, T.C., S.W. and X.W.; Writing—review & editing, N.Y. and X.Z. All authors have read and agreed to the published version of the manuscript.

Funding: This work was supported by the National Key Research and Development Program of China (2019YFC1904304), the Fundamental Research Funds for the Central Universities (2023ZKPYHH05) and the University-Industry Collaborative Education Program of the Ministry of Education of China (202101255047).

Institutional Review Board Statement: Not applicable.

Informed Consent Statement: Not applicable.

Data Availability Statement: Some or all data, models, or codes that support the findings of this study are available from the corresponding author upon reasonable request.

Acknowledgments: The authors are grateful to the School of Chemical and Environmental Engineering, China University of Mining and Technology (Beijing), for the experimental equipment and technical support.

Conflicts of Interest: The authors declare no conflicts of interest.

References

1. ACI 229R-13 Report on Controlled Low-Strength Materials; ACI Committee 229; American Concrete Institute: Farmington Hills, MI, USA, 2013.
2. Türkel, S. Strength properties of fly ash based controlled low strength materials. *J. Hazard. Mater.* **2007**, *147*, 1015–1019. [[CrossRef](#)]
3. Liu, Y.L.; Su, Y.P.; Xu, G.Q.; Chen, Y.H.; You, G.S. Research progress on controlled low-strength materials: Metallurgical waste slag as cementitious materials. *Materials* **2022**, *15*, 727. [[CrossRef](#)]
4. Blanco, A.; Pujadas, P.; Cavalaro, S.H.P.; Aguado, A. Methodology for the design of controlled low-strength materials. Application to the backfill of narrow trenches. *Constr. Build. Mater.* **2014**, *72*, 23–30. [[CrossRef](#)]
5. Dinh, B.H.; Kim, Y.S.; Yoon, S. Experimental and numerical studies on the performance of horizontal U-type and spiral-coil-type ground heat exchangers considering economic aspects. *Renew. Energy* **2022**, *186*, 505–516. [[CrossRef](#)]
6. Lee, K.J.; Kim, S.K.; Lee, K.H. Flowable backfill materials from bottom ash for underground pipeline. *Materials* **2014**, *7*, 3337–3352. [[CrossRef](#)] [[PubMed](#)]
7. Wang, C.X.; Liu, Y.; Hu, H.; Li, Y.Y.; Lu, Y. Study on filling material ratio and filling effect: Taking coarse fly ash and coal gangue as the main filling component. *Adv. Civ. Eng.* **2019**, *2019*, 2898019. [[CrossRef](#)]
8. Okuyucu, O.; Jayawickrama, P.; Senadheera, S. Mechanical properties of steel fiber reinforced self-consolidating controlled low strength material for pavement base layers. *J. Mater. Civ. Eng.* **2019**, *31*, 04019177. [[CrossRef](#)]
9. Alizadeh, V.; Helwany, S.; Ghorbanpoor, A.; Sobolev, K. Design and application of controlled low strength materials as a structural fill. *Constr. Build. Mater.* **2014**, *53*, 425–431. [[CrossRef](#)]
10. Alizadeh, V. Finite element analysis of controlled low strength materials. *Front. Struct. Civ. Eng.* **2019**, *13*, 1243–1250. [[CrossRef](#)]
11. Chang, G.F.; Hua, X.Z.; Liu, X.; Li, C.; Wang, E.Q.; Sun, B.J. Fluidity influencing factor analysis and ratio optimization of new filling slurry based on the response surface method. *J. Renew. Mater.* **2022**, *10*, 1439–1458. [[CrossRef](#)]
12. Li, J.Y.; Wang, J.M. Comprehensive utilization and environmental risks of coal gangue: A review. *J. Clean. Prod.* **2019**, *239*, 117946. [[CrossRef](#)]
13. Kerimkulova, A.R.; Azat, S.; Velasco, L.; Mansurov, Z.A.; Lodewyckx, P.; Tulepov, M.I.; Kerimkulova, M.R.; Berezovskaya, I.; Imangazy, A. Granular rice husk-based sorbents for sorption of vapors of organic and inorganic matters. *J. Chem. Technol. Metall.* **2019**, *54*, 578–584.
14. Tauanov, Z.; Azat, S.; Baibatyrova, A. A mini-review on coal fly ash properties, utilization and synthesis of zeolites. *Int. J. Coal Prep. Util.* **2020**, *42*, 1968–1990. [[CrossRef](#)]
15. Kaliyavaradhan, S.K.; Ling, T.C.; Guo, M.Z. Upcycling of wastes for sustainable controlled low-strength material: A review on strength and excavatability. *Environ. Sci. Pollut. Res.* **2022**, *29*, 16799–16816. [[CrossRef](#)] [[PubMed](#)]

16. Siddique, R. Utilization of waste materials and by-products in producing controlled low-strength materials. *Resour. Conserv. Recycl.* **2009**, *54*, 1–8. [[CrossRef](#)]
17. Ling, T.C.; Kaliyavaradhan, S.K.; Poon, C.S. Global perspective on application of controlled low-strength material (CLSM) for trench backfilling—An overview. *Constr. Build. Mater.* **2018**, *158*, 535–548. [[CrossRef](#)]
18. Ibrahim, M.; Rahman, M.K.; Najamuddin, S.K.; Alhelal, Z.S.; Acero, C.E. A review on utilization of industrial by-products in the production of controlled low strength materials and factors influencing the properties. *Constr. Build. Mater.* **2022**, *325*, 126704. [[CrossRef](#)]
19. Cheng, B.C.; Liu, R.T.; Li, X.H.; Castillo, E.D.R.; Chen, M.J.; Li, S.C. Effects of fly and coal bottom ash ratio on backfill material performance. *Constr. Build. Mater.* **2022**, *319*, 125831. [[CrossRef](#)]
20. Kuo, W.T.; Wang, H.Y.; Shu, C.Y.; Su, D.S. Engineering properties of controlled low-strength materials containing waste oyster shells. *Constr. Build. Mater.* **2013**, *46*, 128–133. [[CrossRef](#)]
21. Zhen, G.Y.; Lu, X.Q.; Zhao, Y.C.; Niu, J.; Chai, X.L.; Su, L.H.; Li, Y.Y.; Liu, Y.; Du, J.R.; Hojo, T.; et al. Characterization of controlled low-strength material obtained from dewatered sludge and refuse incineration bottom ash: Mechanical and microstructural perspectives. *J. Environ. Manag.* **2013**, *129*, 183–189. [[CrossRef](#)]
22. Das, S.K.; Mahamaya, M.; Reddy, K.R. Coal mine overburden soft shale as a controlled low strength material. *Int. J. Min. Reclam. Environ.* **2020**, *34*, 725–747. [[CrossRef](#)]
23. Chen, H.J.; Lin, H.C.; Tang, C.W. Application of the Taguchi method for optimizing the process parameters of producing controlled low-strength materials by using dimension stone sludge and lightweight aggregates. *Sustainability* **2021**, *13*, 5576. [[CrossRef](#)]
24. Katz, A.; Kovler, K. Utilization of industrial by-products for the production of controlled low strength materials (CLSM). *Waste Manag.* **2004**, *24*, 501–512. [[CrossRef](#)] [[PubMed](#)]
25. Fang, X.L.; Wang, L.; Poon, C.S.; Baek, K.; Tsang, D.C.W.; Kwok, S.K. Transforming waterworks sludge into controlled low-strength material: Bench-scale optimization and field test validation. *J. Environ. Manag.* **2019**, *232*, 254–263. [[CrossRef](#)] [[PubMed](#)]
26. Xiao, R.; Polaczyk, P.; Jiang, X.; Zhang, M.M.; Wang, Y.H.; Huang, B.S. Cementless controlled low-strength material (CLSM) based on waste glass powder and hydrated lime: Synthesis, characterization and thermodynamic simulation. *Constr. Build. Mater.* **2021**, *275*, 122157. [[CrossRef](#)]
27. Ricardo, S.; Jacob, H.; Jeffery, R.; David, L. Relative proportioning method for controlled low-strength material. *ACI Mater. J.* **2015**, *112*, 179–188. [[CrossRef](#)]
28. Lan, W.; Wu, A.; Yu, P. Development of a new controlled low strength filling material from the activation of copper slag: Influencing factors and mechanism analysis. *J. Clean. Prod.* **2020**, *246*, 119060. [[CrossRef](#)]
29. ASTM D6103-17; Standard Test Method for Flow Consistency of Controlled Low Strength Materials (CLSM). ASTM: West Conshohocken, PA, USA, 2017.
30. GB/T 50080-2016. Standard for Test Method of Performance on Ordinary Fresh Concrete. Ministry of Housing and Urban-Rural Development of the People's Republic of China and General Administration of Quality Supervision, Inspection and Quarantine of the People's Republic of China: Beijing, China, 2016.
31. ASTM D6023-2016; Standard Test Method for Density (Unit Weight), Yield, Cement Content, and Air Content (Gravimetric) of Controlled Low-Strength Material (CLSM). ASTM: West Conshohocken, PA, USA, 2016.
32. GB/T 50081-2019; Standard for Test Method of Concrete Physical and Mechanical Properties. Ministry of Housing and Urban-Rural Development of the People's Republic of China and State Administration for Market Regulation: Beijing, China, 2019.
33. HJ 557-2010; Solid Waste-Extraction Procedure for Leaching Toxicity-Horizontal Vibration Method. Ministry of Environment Protection of the People's Republic of China: Beijing, China, 2010.
34. Amer, I.; Kohail, M.; El-Feky, M.S.; Rashad, A.; Khalaf, M.A. Characterization of alkali-activated hybrid slag/cement concrete. *Ain Shams Eng. J.* **2021**, *12*, 135–144. [[CrossRef](#)]
35. Shi, Y.B.; Ye, Y.C.; Hu, N.Y.; Huang, X.; Wang, X.H. Experiments on material proportions for similar materials with high similarity ratio and low strength in multilayer shale deposits. *Appl. Sci.* **2021**, *11*, 9620. [[CrossRef](#)]
36. Li, Y.H.; Bai, J.B.; Liu, L.M.; Wang, X.Y.; Yang, Y.; Li, T. Micro and macro experimental study of using the new cement-based self-stress grouting material to solve shrinkage problem. *J. Mater. Res. Technol.* **2022**, *17*, 3118–3137. [[CrossRef](#)]
37. Mneina, A.; Soliman, A.M.; Ahmed, A.; El Naggar, M.H. Engineering properties of controlled low-strength materials containing treated oil sand waste. *Constr. Build. Mater.* **2018**, *159*, 277–285. [[CrossRef](#)]
38. Sivakumar, N.; Hashim, A.R.; Nadzriah, A.H.S. Effect of quarry dust addition on the performance of controlled low-strength material made from industrial waste incineration bottom ash. *Int. J. Miner. Metall. Mater.* **2012**, *19*, 536–541. [[CrossRef](#)]
39. Poon, C.S.; Lam, L.; Kou, S.C.; Wong, Y.L.; Wong, R. Rate of pozzolanic reaction of metakaolin in high-performance cement pastes. *Cem. Concr. Res.* **2001**, *31*, 1301–1306. [[CrossRef](#)]
40. Cho, Y.K.; Jung, S.H.; Choi, Y.C. Effects of chemical composition of fly ash on compressive strength of fly ash cement mortar. *Constr. Build. Mater.* **2019**, *204*, 255–264. [[CrossRef](#)]
41. Zhang, J.X.; Wang, J.G.; Li, X.H.; Zhou, T.J.; Guo, Y.Y. Rapid-hardening controlled low strength materials made of recycled fine aggregate from construction and demolition waste. *Constr. Build. Mater.* **2018**, *173*, 81–89. [[CrossRef](#)]
42. Cong, M.L.; Zhang, S.S.; Sun, D.D.; Zhou, K.P. Optimization of preparation of foamed concrete based on orthogonal experiment and range analysis. *Front. Mater.* **2021**, *8*, 778173. [[CrossRef](#)]

43. Wei, Z.; Yang, K.; He, X.; Zhang, J.Q.; Hu, G.C. Experimental study on the optimization of coal-based solid waste filling slurry ratio based on the response surface method. *Materials* **2022**, *15*, 5318. [[CrossRef](#)] [[PubMed](#)]
44. GB 5085.3-2007; Identification Standards for Hazardous Wastes-Identification for Extraction Toxicity. State Environmental Protection Administration, and General Administration of Quality Supervision, Inspection and Quarantine of the People's Republic of China: Beijing, China, 2007.
45. Xin, J.; Liu, L.; Xu, L.H.; Wang, J.Y.; Yang, P.; Qu, H.S. A preliminary study of aeolian sand-cement-modified gasification slag-paste backfill: Fluidity, microstructure, and leaching risks. *Sci. Total Environ.* **2022**, *830*, 154766. [[CrossRef](#)] [[PubMed](#)]
46. Chen, Q.Y.; Hills, C.D.; Tyrer, M.; Slipper, I.; Shen, H.G.; Brough, A. Characterization of products of tricalcium silicate hydration in the presence of heavy metals. *J. Hazard. Mater.* **2007**, *147*, 817–825. [[CrossRef](#)] [[PubMed](#)]

Disclaimer/Publisher's Note: The statements, opinions and data contained in all publications are solely those of the individual author(s) and contributor(s) and not of MDPI and/or the editor(s). MDPI and/or the editor(s) disclaim responsibility for any injury to people or property resulting from any ideas, methods, instructions or products referred to in the content.